

Negative-ion formation in electron-stimulated desorption of CF_2Cl_2 adsorbed on Ru(0001)

Q.-B. Lu, Z. Ma, and Theodore E. Madey

Laboratory for Surface Modification and Department of Physics and Astronomy, Rutgers, The State University of New Jersey, Piscataway, New Jersey 08854-8019

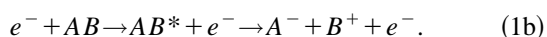
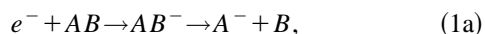
(Received 22 May 1998)

Electron-stimulated desorption of F^- and Cl^- from CF_2Cl_2 adsorbed on Ru(0001) at 25 K has been studied. For an electron energy of 100 eV, the F^- yield exhibits a maximum at nearly the first monolayer, while the Cl^- yield is strongly quenched for coverages below 1 ML and remains much lower than the F^- yield for all coverages measured (0–5 ML). A molecular orientation effect may explain the preferential quenching of Cl^- for coverages ≤ 1 ML. However, trapping of low-energy Cl^- ions at the surface due to an image/polarization potential and charge-transfer deexcitation of intermediate excited molecular states is most likely responsible for the low Cl^- yield at all coverages. It is suggested that the decrease of F^- and Cl^- with higher coverages may be connected with a decrease in secondary electron transmission to the outermost CF_2Cl_2 layer. Moreover, for a multilayer covered surface, a broad peak associated with Cl^- emission is observed at an electron energy around 18.5–20 eV. This feature is assigned to a core-excited negative-ion resonance. This resonance is believed to be formed via an electronic excitation of the molecule by an incident electron followed by capture of a secondary electron from the substrate to the excited molecule. [S0163-1829(98)00948-5]

I. INTRODUCTION

The study of chlorofluoromethanes (freons) has received continued interest because of their industrial applications and their well-known association with the ozone depletion in the upper atmosphere.^{1,2} It has been proposed that these compounds released into the upper atmosphere destroy the ozone layer via a halogen-oxygen-reaction chain with halogen atoms created by photodissociation or electron-impact-induced dissociation of the freons.^{1,2} Moreover, freon-11 (CFCl_3) and freon-12 (CF_2Cl_2) have been used routinely as tracers in studies of ocean circulation and mixing processes.³ Since the concentrations of freons in the upper atmosphere have rapidly increased over the last three decades,³ investigation of their dissociation by photoreactions or electron impact is a matter of widespread concern.

Negative ions are the dominant products observed upon low-energy electron impact with gas-phase, condensed-phase and adsorbed halomethanes;^{4,5} negative ions are also observed in photoinduced dissociation of halomethanes adsorbed on metallic surfaces via attachment of photoexcited substrate electrons.⁶ It is well established^{5–10} that the basic processes for negative ion formation on solid surfaces are closely related to the corresponding processes known from gas-phase reactions. For a diatomic molecule AB , these processes are represented by



Equations 1(a) and 1(b) are referred to as dissociative electron attachment (DEA) and dipolar dissociation (DD), respectively. In DEA, an incident electron is temporarily captured by a molecule to form a transient negative ion (TNI) (AB^-), which can involve either a single-electron resonance associated with the ground electronic state or a core-excited

resonance with an electronically excited state of the neutral molecule (the ‘‘parent’’).⁹ For the latter case, the resonance is a two-electron, one-hole configuration that is classified either as a Feshbach resonance or a core-excited shape resonance, dependent on its energy relative to the parent state. If the lifetime of the TNI is comparable to the vibrational period of the molecule, then dissociation into a stable anion and a neutral fragment can take place. DEA processes occur generally at electron energies less than 15 eV, while thresholds for DD are higher, typically ≥ 15 eV.

Investigation of anion formation has been extended to molecular films and adsorbed systems.^{5–8,11} F^- , Cl^- , H^- , and D^- yields in electron-stimulated desorption (ESD) of adsorbed layers or films have been reported for PF_3 and CCl_4 ,^{12–14} $\text{D}_2\text{O}(\text{H}_2\text{O})$,^{15,16} CF_4 , CDCl_3 , CD_2Cl_2 , CH_3Cl , and CH_3Br ,⁵ CFCl_3 ,¹⁷ CF_3Cl ,¹⁸ and in photon stimulated desorption (PSD) for CCl_4 , CHCl_3 , CH_2Cl_2 , and CCl_3Br ,⁶ respectively. The results are generally analogous to the gas-phase data. In the condensed phase, however, DEA and DD processes can be significantly modified due to the existence of surrounding molecules and the metallic substrate. For instance, Sanche and co-workers¹⁹ observed features in electron-stimulated desorption of O^- from a condensed O_2 film, which involve symmetry-forbidden transitions in gas-phase O_2 molecules. More recently, Meinke and Illenberger¹⁷ reported a preferential quenching of Cl^- desorption via DEA in ESD of condensed and adsorbed CFCl_3 in the electron energy range of 0–15 eV which was attributed to the substrate-induced image potential and molecular-orientation effects.

When a metallic substrate containing an adsorbed layer of molecules is irradiated by an electron beam of an energy higher than tens of eV, a large number of low-energy secondary electrons can be created. The maxima of secondary electron yields are around 1–2 for most transition-metal substrates,²⁰ and may become higher with deposition of a dielectric-molecular layer.¹³ The energy distribution of secondary electrons is normally rather broad and exhibits a

maximum at a few eV. As a consequence, DEA may play an important role in negative ion formation even with an incident electron beam of an energy higher than the threshold for DD. This can be the case especially for adsorbed halomethanes because they generally have resonance energy levels in the range from zero to a few eV and have large electron affinities.^{4,8} As recently reviewed by Sanche,⁷ much of the damage caused by electron-beam irradiation of condensed molecular layers may be due to DEA processes. Moreover, desorption of negative ions in UV laser irradiation at 193–248 nm (4.4–6.4 eV) of halomethanes adsorbed on Ag(111) provides direct evidence for DEA processes due to photoinduced transfer of substrate electrons to molecules.⁶

The presence of a metallic substrate also induces an image potential on both the intermediate AB^- state and the departing A^- fragment. The resulting ions can escape from the surface only if their kinetic energy surmounts the image/polarization potential that is typically of the order of 0.5–1.5 eV. In DEA, the conservation of energy and momentum for the dissociation of AB^- [Eq. 1(a)] gives the kinetic energy E_k of the departing anion (A^-) fragment by⁵

$$E_k = (1 - \mu)[E_i - D(B-A) + E_a(A) - E^* + E_{\text{pol}}] - E_{\text{pol}}, \quad (2)$$

where μ is the mass ratio of the A^- fragment to the parent AB molecule, E_i is the energy of incident electrons at the resonance (the resonance energy), E^* is the total internal energy retained by the fragments, $D(B-A)$ the dissociation energy, E_a is the electron affinity of the fragment A , and E_{pol} is the image/polarization potential induced by the substrate. A large mass of A will result in a unfavorable factor ($1 - \mu$) for the departing A^- ; this has been proposed to be the major factor leading to the low Cl^- or Br^- yield in ESD of CCl_4 , CDCl_3 , CD_2Cl_2 , CH_3Cl , and CH_3Br on Pt,⁵ CFCl_3 on Au,¹⁷ and in PSD of CH_3Cl on Ni(111) (Ref. 21) via DEA processes associated with low-energy negative-ion resonances. In contrast, the image potential effect should have a minor effect on the A^- yield via DEA with higher-energy resonances or via DD, since the higher kinetic energy of A^- is generally sufficient to overcome the image potential. In any case, however, the image potential will modify the kinetic energy of the departing A^- .

Furthermore, when an excited atomic or molecular state is on or near a metallic surface, strong quenching due to charge transfer from the substrate is generally expected. Auger and resonant deexcitation are two typical charge-transfer processes, as have been demonstrated in metastable deexcitation spectroscopy (MDS) (Ref. 22) and in surface photochemistry.²³

In experiments with CF_2Cl_2 , Illenberger and co-workers^{4,8} have studied anion formation via DEA in electron impact of the gas and ESD of the condensed molecular film. For both phases, they observe a resonance at a very low-electron energy associated entirely with Cl^- formation; in earlier work,^{4,8} the Cl^- resonance was found at an electron of about 0.8 eV, but a more recent study²⁴ with a higher-energy resolution shows that the low-energy resonance associated with Cl^- desorption appears close to zero eV. Another resonance is found for both phases around 3.0 eV coupled entirely with emission of F^- . However, the dominant negative ion product

is Cl^- for the gas phase (the intensity ratio of Cl^- to F^- is approximately 8:1), while for the condensed phase the F^- yield is higher (Cl^- : $\text{F}^- = 1:8$). The resonances near 0 eV and at 3.0 eV are assigned to the formation of ground-state TNI's, i.e., single-electron resonances.⁴ Moreover, they observe an additional resonance associated with Cl^- emission with a broad-energy width peaked at about 7.0 eV, uniquely for the condensed phase. The intensity of this resonance is much stronger than that of the low-energy resonance near 0 eV. The higher-energy resonance at 7.0 eV is attributed to an involvement of the first electronically excited state of the molecule,⁸ based on the fact that the width and energy position of the Cl^- yield resembles the first absorption band of CF_2Cl_2 .²

The present effort is part of a program to study the desorption mechanisms and the “depth of origin” for positive and negative halogen ions in ESD of halogen-containing molecules on metal surfaces. In this paper, we present a study of negative-ion formation in low-energy (15–300 eV) electron stimulated desorption from CF_2Cl_2 molecules adsorbed on Ru(0001) with coverages from 0 to 5 ML. We find that the F^- yield exhibits a maximum at a coverage near 1 ML, while the Cl^- yield is strongly quenched for coverages below 1 ML and remains much lower than the F^- yield even up to 5 ML (less than 5%). For a multilayer of CF_2Cl_2 , an additional feature coupled with the desorption of Cl^- is observed at an incident electron energy of 18.5–20 eV, which is attributed to the formation of a core-excited TNI state. The preferential quenching of Cl^- on or near the metallic substrate is discussed in terms of molecular orientation, image potential, and charge-transfer effects. These effects are very important in electron-stimulated desorption, surface photochemistry, and interaction of ion/metastable atoms with solid surfaces.

II. EXPERIMENT

The experiments have been conducted, in an ultrahigh vacuum (UHV) chamber that has been described previously.^{12–14} The base pressure of the chamber is 5.0×10^{-11} torr. The chamber is equipped with Auger electron spectroscopy (AES), low-energy electron diffraction (LEED), thermal desorption spectroscopy (TDS), and electron-stimulated desorption-ion angular distribution (ESDIAD) with time-of-flight (TOF) capability for mass- and angle-resolved ion detection. The ESDIAD/TOF detector is composed of four grids, five microchannel plates, and a position-sensitive resistive-anode encode (RAE). The RAE is connected to a position-analyzing computer to obtain a direct acquisition of two-dimensional (2D) digital data. This detector permits a direct measurement of the total yield and the angular distribution of a specific desorbing ion species. The typical counting rate is $3 \times 10^3/\text{s}$.

The Ru(0001) crystal can be cooled to 25 K with a closed-cycle helium refrigerator and heated to 1600 K by electron bombardment. After sputtering using 1-keV Ar^+ and annealing in oxygen, the cleanliness of the surface is checked by AES and LEED. Prior to being introduced into the chamber, CF_2Cl_2 is purified by several freeze-pump-thaw cycles. Its purity is checked by a quadrupole mass spectrometer (QMS) as the gas is introduced into the chamber. CF_2Cl_2

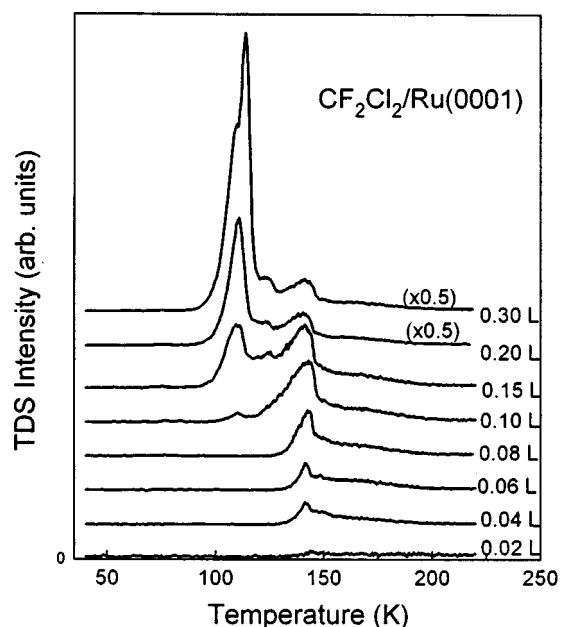


FIG. 1. TDS spectra of CF_2Cl_2 on Ru(0001) at ~ 25 K with increasing exposure, based on detection of CF_2Cl^+ fragment.

and Xe (Matheson, 99.995%) are dosed onto the surface at 25 K with two separate directional dosers. The exposure is measured by a Bayard-Alpert ionization gauge. Here, our dosing is not background exposure, but directional dosing. Thus, the unit Langmuir ($1 \text{ L} = 1 \times 10^{-6} \text{ Torr s}$) is only used as a relative exposure unit. The relative coverages of CF_2Cl_2 and Xe are determined from TDS spectra measured using the QMS, 1 ML is defined as the coverage corresponding to the saturation of the monolayer peak in thermal desorption spectra. For CF_2Cl_2 , 1 ML corresponds to a measured exposure of $\sim 0.1 \text{ L}$. In TDS, the sample is heated by resistive heating, and the heating rate is $\sim 4 \text{ K/s}$.

The electron-beam energy is adjustable from 15 to 1000 eV with an uncertainty within 0.5 eV. The electron gun is typically pulsed at a repetition rate of 30 kHz and a pulse width of 100 ns. The beam size is about 1 mm^2 , and the incident electron flux for one measurement is $< 4 \times 10^{12} \text{ cm}^{-2}$. The low electron flux results in negligible damage to the molecular sample. The flight times for F^- and Cl^- are 1.6 and 2.1 μs , respectively, with a bias voltage of -100 V applied to the sample.

III. RESULTS

The adsorption of CF_2Cl_2 on Ru(0001) is first studied by use of TDS and AES. The TDS spectra of CF_2Cl_2 with various exposures are shown in Fig. 1, based on the detection of CF_2Cl^+ (atom mass = 85 amu), the dominant fragment in the CF_2Cl_2 mass spectrum. It can be seen that a peak at about 140 K grows from the lowest exposures, and becomes saturated for exposures more than 0.1 L. For exposures above 0.1 L a second peak at $\sim 110 \text{ K}$ appears and grows with increasing exposure. The first peak at 140 K and the second peak at 110 K are assigned to the monolayer peak and the multilayer peak, respectively. Between the peaks of the monolayer and the multilayer, a small peak appears at $\sim 120 \text{ K}$; this peak may be connected with a phase transition from the crowded

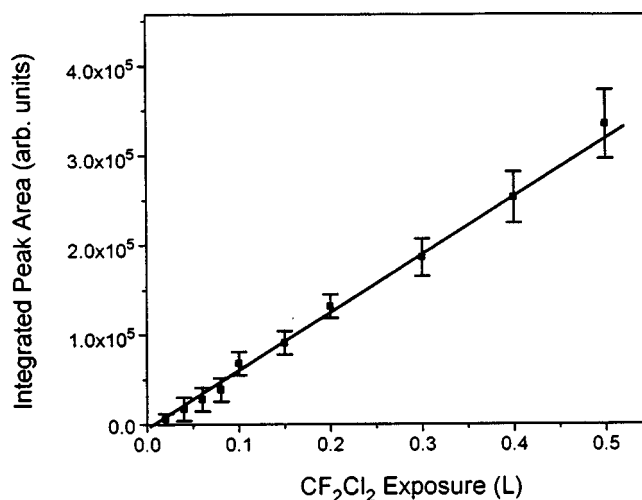


FIG. 2. Total TDS peak area integrated with desorption time as a function of CF_2Cl_2 exposure.

first layer to the multilayer, as seen for Xe adsorption.²⁵ There is also a shoulder seen on the multilayer peak at high exposures, perhaps due to a decrease in binding energy upon completion of the first physisorbed layer. The total peak area integrated with time as a function of CF_2Cl_2 exposure is shown in Fig. 2. One can see that the total peak area increases linearly with increasing CF_2Cl_2 exposure in the range of 0–5 ML, and the exposure “offset” on the extrapolated line is very small. These data indicate that dissociation of CF_2Cl_2 into fragments upon adsorption is very small (less than 0.1 ML), that is, CF_2Cl_2 is mainly molecularly adsorbed on the surface. This conclusion is similar to that reported for CH_3Cl on Ni(111) (Ref. 21) and Al(111),²⁶ CHCl_3 , CH_2Cl_2 , and CH_3Cl on Ag(111),⁶ all of which are found to adsorb in completely molecular form, but different from adsorption of CCl_4 on Ru(0001) (Ref. 13) and Ag(111) (Ref. 6) for which molecules are partially dissociated at fractional monolayer coverages. Further, from the desorption temperature we can estimate the desorption energy corresponding to the multilayer peak to be $0.28 \pm 0.05 \text{ eV}$, in good agreement with the value of 0.27 eV for the heat of vaporization of CF_2Cl_2 .²⁰ Based on the monolayer peak temperature of 140 K, we estimate the desorption energy to be $0.36 \pm 0.05 \text{ eV}$, assuming first-order desorption kinetics and the preexponential factor $\nu = 10^{13} \text{ s}^{-1}$. This indicates that CF_2Cl_2 is weakly bound to the surface.

From the gas-phase data, it is expected that low-energy electron bombardment of a CF_2Cl_2 -adsorbed surface should lead to desorption of F^- and Cl^- , and both ions are observed in our experiments. As shown in Fig. 3, the 2D ESDIAD patterns exhibit only a central beam for both F^- and Cl^- emission, indicating that desorption trajectories are centered along the surface normal. The ion yields for F^- and Cl^- as a function of CF_2Cl_2 coverage are shown in Fig. 4 for bombardment by 100 eV electrons. It can be seen that the F^- yield increases from the lowest coverage, exhibits a maximum ($\sim 6 \times 10^{-7}$ ions/electron) at about 0.8 ML, and then decreases with higher coverages. This behavior is quite similar to that for the Cl^- yield in UV laser irradiation ($h\nu = 4.4\text{--}6.4 \text{ eV}$) of various chloromethanes adsorbed on Ag(111), in which evidence for DEA via capture of photo-



FIG. 3. ESDIAD patterns of F^- (left) and Cl^- (right) from CF_2Cl_2 -covered Ru(0001).

excited substrate electrons to molecules is reported.⁶ The coverage dependence of F^- from ESD of PF_3 adsorbed on Ru(0001) at an incident electron energy $E_i=40$ eV also shows a similar maximum at ~ 1 ML.¹⁴ In addition, a similar dependence of the O^- yield on the Ar spacer thickness has also been reported for a constant O_2 coverage in the $O_2/Ar/Pt$ system at $E_i=30$ or 40 eV.²⁷ On the other hand, it is observed that contrary to the gas-phase data where Cl^- is dominant, the Cl^- yield from adsorbed CF_2Cl_2 is considerably smaller than the F^- yield at all coverages from fractional monolayer to multilayers: an extremely low Cl^- ion yield is detected for coverages below 1 ML, and the yield remains much lower than the F^- yield even for coverages as high as 5 ML (Fig. 4). As mentioned in Sec. I the dominant product is also F^- for the condensed phase.⁸ This result is quite similar to that reported for ESD of $CFCl_3$ on Au in the electron energy of 0–15 eV.¹⁷

We have measured the F^- and Cl^- yields vs incident electron energy for a multilayer of CF_2Cl_2 on Ru(0001). A rare-gas (Xe) spacer layer predosed on the surface is commonly used to isolate effects of the metallic substrate on the molecular excitation.^{7,11,17–19} Shown in Figs. 5(a) and 5(b) are the results for a 5-ML CF_2Cl_2 with 2.5-ML Xe spacer. The lowest-energy electron beam that we could generate with a beam current large enough for negative-ion detection is 15 eV. A broad feature for Cl^- desorption is observed at an electron energy of 18.5–20 eV, and the ratio of Cl^-/F^- exhibits a strong peak at about 19.4 eV. This indicates exist-

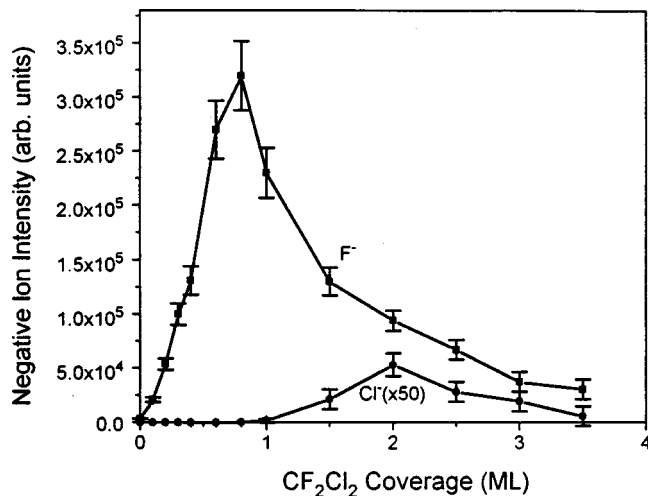


FIG. 4. F^- and Cl^- intensities with 100-eV electrons incident onto Ru(0001) as a function of CF_2Cl_2 coverage.

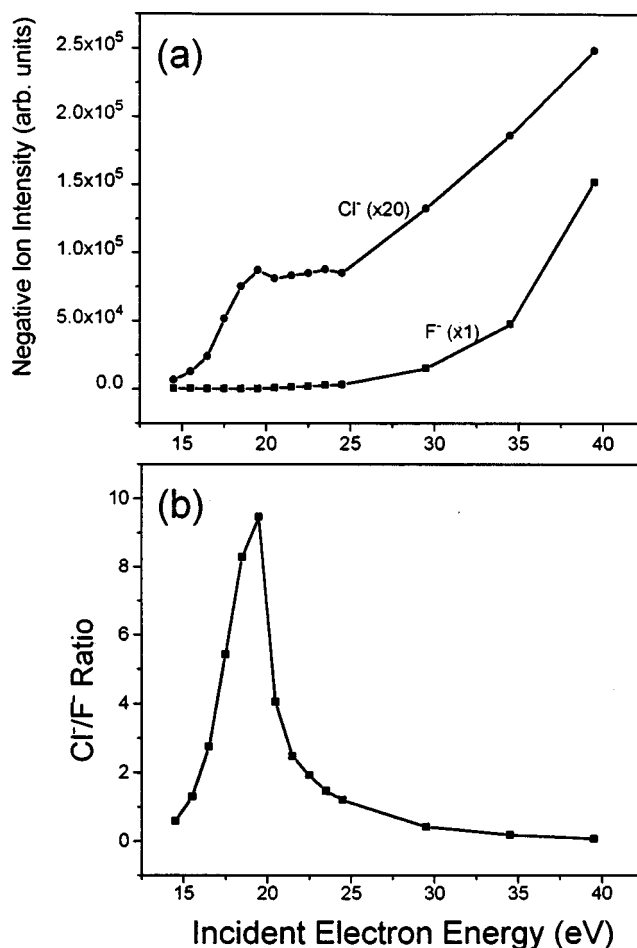


FIG. 5. (a) F^- and Cl^- intensities and (b) the ratio of Cl^-/F^- from 5-ML CF_2Cl_2 on Ru(0001) with 2.5-ML Xe spacer layer vs incident electron energy, after normalization by beam current.

tence of a resonance associated with the emission of Cl^- . This resonance can also be observed for a multilayer of CF_2Cl_2 without a Xe spacer, but the intensity is lower than that with a Xe spacer layer. The higher-energy structure at 18.5–20 eV has not been reported previously, even in the gas-phase experiments.

To elucidate the formation mechanism for this resonance peak, the Cl^- intensity as a function of incident-electron current with the electron energy fixed at 19.4 eV is measured, as shown in Fig. 6. It can be seen that the Cl^- intensity increases linearly with the square of the incident-electron current. The significance of this observation is discussed below.

IV. DISCUSSION

Before we discuss the ESD observations seen here, it is useful to briefly summarize the electronic structure of CF_2Cl_2 . Photoelectron spectra^{28–30} indicate that the highest occupied molecular orbitals lie at binding energies of 12.3, 12.6, 13.2, and 13.5 eV, consisting of the four chlorine lone-pair orbitals. Also, photoabsorption spectra^{2,28} show that the first absorption band is centered at nearly 7.0 eV, which has been assigned to an electronic excitation from the chlorine lone-pair orbitals to the lowest unoccupied molecular orbitals (LUMO) of the C-Cl character.²⁸ This implies that the C-Cl

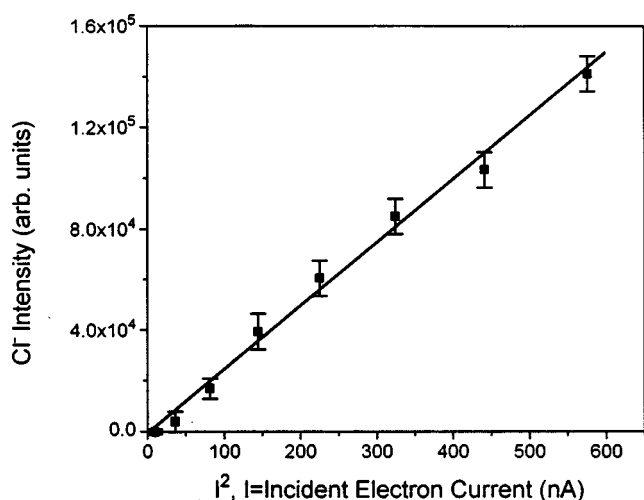


FIG. 6. Cl^- yield at the electron energy of 19.4 eV as a function of I^2 , where I is the electron beam current.

orbitals lie at approximately 6.0 eV in binding energy. Once occupied, the C-Cl orbitals are highly dissociative due to their strongly localized antibonding character.²⁸ There is also a broad photoabsorption band centered at 19.2 eV observed with higher photon energies.³⁰ Interpretation of this electronic excitation is somewhat difficult since there are no photoelectron spectra reported for CF_2Cl_2 at binding energies greater than 22 eV. If we simply ascribe the absorption band to a transition from a deep-valence orbital to the lowest unoccupied C-Cl orbitals, then the deep-valence orbital should lie at about 25.2 eV. This is very likely, as it has been expected that deeper valence orbitals are connected to fluorine lone-pair orbitals or C-F bonding orbitals.^{29,30} For a free F atom, the binding energy of the F 2s level is 31 eV. The F 1s binding energy is expected to be smaller in a CF_2Cl_2 molecule. Moreover, the following ESD results support this assignment.

A. Mechanisms for preferential quenching of Cl^-

First, let us discuss the mechanisms for the preferential quenching of Cl^- on or near the metallic substrate. This is illustrated in Fig. 4, which shows that F^- ESD is considerably more intense than Cl^- ESD over a large range of coverage; in particular, for less than 1 ML the Cl^- signal is barely detectable. One can generally expect that the presence of a metallic substrate will induce such effects as (i) molecular orientation, (ii) image potential, and (iii) modification of the lifetime of excited molecule.^{7,8,11,17,18}

(i) In the gas phase, molecules are oriented randomly, while for molecules adsorbed on a surface, the molecule-substrate interaction may cause specific orientations of adsorbed species. Tetrahedral molecular CF_2Cl_2 is weakly bonded to Ru(0001), as discussed in Sec. III and is expected to adsorb with three ligands close to the surface, and one pointed away. A random distribution of F and Cl among the ligands would lead to equal probability for F and Cl to be pointed away from the surface. If, however, the Cl-Ru interaction energy is stronger than that for F-Ru, there would be a relatively larger fraction of C-Cl bonds pointed towards the surface; a larger fraction of C-F bonds pointed away from the

surface would be expected. If this is the case (and we have no direct evidence for or against), desorption along the surface normal may be seen for both F^- and Cl^- in the first monolayer, but F^- is expected to dominate. On the other hand, a surface-induced orientation effect is generally significant only for coverages up to 1 ML, as molecules adsorb randomly in multilayers. The very low Cl^- yield in comparison with the F^- yield even for coverages up to 5 ML indicates that there exist other mechanisms in addition to possible molecular orientation leading to the preferential quenching of Cl^- ions near the surface.

(ii) A second possible mechanism for quenching of Cl^- involves an image/polarization potential effect. As discussed in the Introduction, image-potential effects may strongly affect the yield of a negative-ion species resulting from a low-energy ground-state resonance. For a CF_2Cl_2 molecule, $D(\text{CFCl}_2\text{-F})=4.93$ eV,⁴ $D(\text{CF}_2\text{Cl-Cl})=3.58$ eV,⁴ $E_a(\text{F})=3.45$ eV, and $E_a(\text{Cl})=3.61$ eV in Eq. (2). With the assumption of $E_{\text{pot}}=1.0$ eV for adsorbed or condensed CF_2Cl_2 , Eq. (2) gives the final kinetic energy $E_k \leq 1.1$ eV for F^- desorption at $E_i=3.0$ eV and $E_k \leq -0.3$ eV for Cl^- at $E_i \approx 0$ eV. The kinetic-energy maximum corresponds to the assumption that the total excess energy liberated in the dissociation is completely transferred into the translation energy of the fragments, that is, the internal energy retained by the fragments is zero ($E^*=0$). These evaluations indicate that the image/polarization potential leads to trapping at the surface of Cl^- ions corresponding to the dissociation of the negative-ion resonance near 0 eV. However, most of the F^- ions resulting from the dissociation of the resonance at 3.0 eV can overcome the attractive potential and desorb from the surface. This prediction is in good agreement with the results observed in condensed phase experiments, where an $\sim 8:1$ ratio of F^-/Cl^- is seen.⁸ The condensed phase results also shows a Cl^- peak at $E_i \sim 7.0$ eV, whose intensity is much stronger than that of the Cl^- peak at nearly 0 eV. A higher Cl^- yield would be expected from resonances at 7.0 and 19.4 eV if only the image potential were effective. In the present experiments, the fact that the Cl^- yield remains very low even for coverages up to 5 ML and for an incident electron energy of 19.4 eV suggests the existence of another mechanism responsible for the preferential quenching of Cl^- ions.

(iii) As mentioned in the Introduction, for DEA connected with a core-excited resonance or for DD, the formation of negative ions involves an intermediate excited-molecular state. This leads to the suggestion that charge-transfer processes may affect the lifetime of the excited-molecular state. Auger and resonant charge-transfer processes are two probable interactions between an electronically excited neutral molecule and a metallic substrate, as schematically shown in Fig. 7. For a simplifying approximation, the excited molecule is assumed to have two nondegenerate electronic levels. The hole is located in a deep valence orbital, while the excited electron occupies the LUMO of the molecule. The excited molecule may be deexcited via an Auger transition of a metal electron to the hole with emission of the excited electron into the vacuum [Auger deexcitation (AD)]. An equivalent process is that the excited electron decays into the hole in the deep valence level of the molecule, while one conduction electron in the metal is emitted into the vacuum with the excess energy. Resonant deexcitation proceeds via

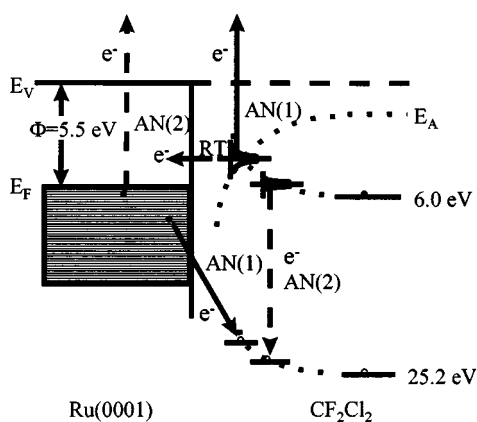


FIG. 7. Schematic energy diagram for the decay of a $[\text{CF}_2\text{Cl}_2]^*$ molecule near a metal surface by RT and AD processes. An AD process can be either a transition of a metal conduction electron to the hole in the deep valence level of the molecule followed by emission of the excited electron into the vacuum [the solid lines, AN(1)] or a decay of the excited electron into the hole with emission of a metal electron into the vacuum [the dashed lines, AN(2)]. Also shown is the shift of the affinity level E_A of the molecule.

resonant tunneling (RT) of the excited electron to the substrate, accompanied by an Auger neutralization of the resulting ion. The work function of the clean Ru(0001) is ~ 5.5 eV.³¹ Thus, the first excited level (LUMO) lies about 0.5 eV below the Fermi level for a free CF_2Cl_2 molecule. This level, however, will shift upwards when the molecule is near the metallic substrate because of the image potential effect.³² Besides the shifting, the excited level is also broadened due to overlap between the metallic and molecular wave functions.³² Both effects are shown schematically in Fig. 7. Resonant deexcitation can occur when the excited level is above the Fermi level. Consequently, both Auger and resonant-electron transfer processes may lead to the deexcitation of the excited molecule prior to attachment of an extra electron to form a negative-ion resonance (DEA) or before dissociation (DD). This effect has been emphasized in surface photochemistry.²³ It should be noted that for a thick molecular-layer covered substrate, RT is strongly suppressed, but AD involving electron transfer from the molecular film is still effective.²² The charge-transfer deexcitation should lead to no preferential quenching of Cl^- or F^- in DD processes. In DEA, however, the F^- yield is associated with the ground-state $[\text{CF}_2\text{Cl}_2]^-$ resonance at ~ 3.0 eV, while the Cl^- yield may result from not only the ground-state resonance close to 0 eV but the core-excited resonances at 7.0 and 19.4 eV. All these resonances are probable for incidence of a high-energy electron beam because of the production of secondary electrons that have a broad-energy distribution. Thus, the above charge-transfer deexcitation does not affect the formation of F^- via DEA, but does affect the formation of Cl^- associated with core-excited resonances. We therefore conclude that the charge-transfer deexcitation may be responsible for the preferential quenching of Cl^- ions associated with core-excited negative ion resonances.

B. Coverage dependence of F^- and Cl^-

Now, we discuss the dependence of the F^- and Cl^- yields on CF_2Cl_2 coverage, as shown in Fig. 4. In the literature,

there have been several reports of coverage-dependent negative-ion yields, which display a maximum at ~ 1 ML, with different interpretations. Negative ion formation from molecules adsorbed on a metallic substrate with an incident electron energy greater than tens of eV has been attributed primarily to DD processes, and the appearance of the yield maximum at one monolayer was interpreted as due to a substrate-induced increase of the kinetic energy of the departing ion via DD, and hence the escape probability.^{14,27} It was also assumed^{14,27} that at low coverages, deexcitation of the intermediate AB^{*-} in DEA is more effective than that of the neutral AB^* state in DD as the image potential attracts the former towards the substrate. Consequently, strong quenching of negative-ion formation via DEA would be expected at coverages ≤ 1 ML. On the other hand, it has also been observed that the negative ion (X^-) yield via DEA exhibits a maximum at the first-molecular monolayer in (UV) laser irradiation of a series of halomethanes (RX , $X = \text{halogen}$) such as CCl_4 , CHCl_3 , CH_2Cl_2 , and CH_3Cl adsorbed on metallic surfaces.⁶ This has been attributed to the addition of extra kinetic energy to the desorbing ion from the chemical reaction of R with the substrate, thus enhancing the escape probability of X^- .⁶

Obviously, there is disagreement between the above two mechanisms. In considering the former mechanism, we note that (i) it is difficult to explain the strong preferential quenching of Cl^- even for coverages up to 5 ML. As mentioned above, desorption via DD should not lead to a preferential quenching of either F^- or Cl^- . (ii) For incident electron-beam energies higher than tens of eV, DD is not the only process, but rather DEA may make a significant contribution to the desorbing ion yield due to the existence of a large number of secondary electrons. (iii) In DD or in DEA with core-excited resonances, strong quenching of the intermediate excited neutral AB^* state at or near a metallic substrate can be expected, without the necessity of an image-potential attraction towards the substrate. This, in fact, has been well verified in metastable deexcitation spectroscopy experiments using a metastable particle (e.g., He^*) as projectile, in which strong deexcitation occurs when the projectile is rather far (3–5 Å) from the adsorbed overlayer.^{22,33} For DEA with a ground-state single-electron resonance, however, the lifetime of AB^- at a metallic substrate can be longer than of AB^* or AB^{*-} , since its electron affinity is increased by the image potential (see Fig. 7) and there is no hole in the valence level (thus, no AD), unlike a core-excited state. Thus, DEA with a ground-state resonance can lead to a high negative-ion yield at low coverages, if the kinetic energy of the departing ion is sufficient to overcome the image potential. This turns out to be the case for the UV irradiation experiments of Ref. 6 and may be the explanation for the present results of F^- from ESD of adsorbed CF_2Cl_2 . As for the chemical reaction enhanced mechanism, the extra kinetic energy from the reaction with the substrate could be important for heavier desorbing ions (e.g., Cl^-), but it should be less efficient for light ions such as F^- that have a kinetic energy large enough to escape even without the extra energy. Moreover, this mechanism cannot explain the dependence of the O^- yield on the Ar spacer thickness in the $\text{O}_2/\text{Ar}/\text{Pt}$ system,²⁷ which also shows a maximum at ~ 1 ML Ar.

As discussed above in Sec. IV A, the appearance of the F^- yield maximum at nearly one monolayer may be due to a molecular orientation effect caused by the metallic substrate. For the first monolayer, one F atom in an adsorbed CF_2Cl_2 molecule may be directed outwards and along the surface normal. The F^- ion has, therefore, a larger probability for departure from the surface. With coverages more than one monolayer, the average orientation of molecules becomes random and is expected to decrease the desorption efficiency of F^- , and increase the desorption of Cl^- . However, it is seen that the Cl^- yield peaks at about 2 ML and then decreases with increasing coverage. Moreover, for chloromethanes such as CCl_4 , $CHCl_3$, CH_2Cl_2 , and CH_3Cl adsorbed surfaces, more Cl atoms may be oriented towards the substrate for the first monolayer than for higher coverages.⁶ The orientation effect would result in a lower desorption efficiency of Cl^- for coverages less than one monolayer and a high efficiency for coverages more than one monolayer. This is inconsistent with what is observed for these molecules.

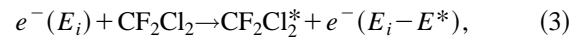
If DEA processes contribute significantly to the formation of Cl^- and F^- ions even for irradiation by 100 eV electrons, then the decrease of the F^- and Cl^- yields at higher coverages may be due to a lowering in transmission of low-energy secondary electrons to the resonance levels in the topmost CF_2Cl_2 layer. The appearance of the Cl^- yield maximum at the coverage of nearly 2 ML can be explained as due to a competing result between the substrate-induced quenching effect discussed above and the transport of secondary electrons to the molecular layer. This suggestion can give a reasonable explanation not only for the present results, but for the similar results on adsorbed halomethanes in UV irradiation.⁶ This suggestion, however, is not conclusive, and further experimental tests may be of interest. We note that in UV irradiation experiments, the variation of the Cl^- yield does not simply follow the change of the photoemission yield.⁶ However, it is known that photoemission from a solid can be well described as a three-step model: photoexcitation in solid, transport of the photoexcited electron to the surface, and escape of the electron across the surface-vacuum barrier.³⁴ Thus, the yield of photoelectrons emitted into the vacuum may not exactly correspond to the true flux of photoexcited electrons transferred to the outermost molecular layer. Indeed, the adsorption of a molecular overlayer may lead to a decrease of the vacuum barrier,²⁶ even formation of a negative-electron-affinity surface.³⁵ This can greatly enhance the photoelectron or secondary-electron yield due to an increase of the escape probability, but it does not mean that the flux of substrate electrons transferred to the molecular layer must increase.

C. Formation of a core-excited negative ion resonance at ~ 19 eV

Finally, we discuss the newly observed higher-energy resonance at ~ 19 eV. Identification of negative-ion resonances in ESD at energies ≥ 15 eV is not well established. Recently, Orlando and co-workers^{15,16} observed a broad structure centered at about 25 eV both in the D_2^- yield and in the D^- yield in ESD of amorphous D_2O ice. They attributed the higher-energy feature to a negative-ion resonance associated with a hole in the deep $2a_1$ valence orbital and two

electrons in the lowest unoccupied $3s:4a_1$ orbital. In fact, core-excited negative-ion resonances associated with electronic excitations from nearly all occupied valence levels to the lowest unoccupied $3s:4a_1$ level of D_2O (H_2O) have been found.^{15,16} Using a similar model, we attribute the higher-energy structure at 18.5–20 eV to a resonance associated with the electronically excited state of CF_2Cl_2 at 19.2 eV.³⁰ This is described as a core-excited negative-ion resonance with a hole in a deep valence orbital probably of F $2s$ character, and two electrons in the lowest unoccupied C-Cl orbital. Like the resonance at ~ 7.0 eV, this higher-energy resonance is highly dissociative and leads to emission of Cl^- ions from the surface due to the strong antibonding character of C-Cl orbitals. Also, it is observed that the Cl^- yield at an electron energy of ~ 19 eV is proportional to the square of the incident current, I^2 (Fig. 6).

After identifying the higher-energy resonance at ~ 19 eV, we discuss several possible scenarios for the formation of $[CF_2Cl_2]^*^-$. First, we note that the formation of higher-energy negative-ion resonances has been associated with multiple scattering of incident electrons.^{7,8} This process could proceed by inelastic scattering of an incident electron at a molecule on the surface, and then the scattered electron with an energy loss is resonantly attached to a second molecule that dissociates. The reaction path can be expressed as

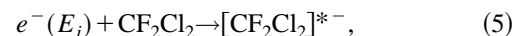


followed by



Here, it is worth noting that the resulting Cl^- would have a very low escape probability due to the image/polarization potential effect, since it is known that the $[CF_2Cl_2]^-$ resonance is close to 0 eV. Moreover, the above processes would also lead to a much lower cross section for the Cl^- peak due to a higher-electron energy ‘‘resonance’’ than that for the Cl^- peak resulting directly from the ground-state resonance with a low-energy incident electron. The reason is that the former involves the cross section of the electronic excitation [Eq. (3)]. However, the condensed phase results show that the Cl^- peak at 7.0 eV is much stronger than that close to 0 eV,⁸ indicating that the Cl^- ion arising from the higher-energy resonance has a larger escape probability.

An alternative path is that the incoming electron, after experiencing the inelastic scattering, backscatters from surrounding molecules, and finally interacts further with the first excited molecule during its limited lifetime, forming an excited negative-ion resonance, that is,



if the intermediate process is omitted. It should be noted that in the above two reaction paths, only one incident electron is involved in formation of a $[CF_2Cl_2]^-$ or $[CF_2Cl_2]^*^-$ transient state. This would lead to a linear dependence of the resonance intensity (and, thus, the Cl^- yield) on incident-electron current. This is inconsistent with the quadratic current dependence of the Cl^- yield, as shown in Fig. 6. This implies that two electrons are involved in the ion formation and desorption. Here, a likely process is that following the

inelastic scattering [Eq. (3)], the excited $[\text{CF}_2\text{Cl}_2]^*$ molecule captures one secondary electron, i.e.,



This event should have a high probability due to the large number of secondary electrons available at the surface. Moreover, dissociation of the core-excited negative-ion resonance will produce a Cl^- ion of a higher-kinetic energy and thus of a higher-escape probability than that from a ground-state resonance. Most significantly, this mechanism is supported by the fact that the Cl^- intensity at the resonance energy depends linearly on the square of the incident current (Fig. 6). One can expect that the probability of Cl^- desorption is proportional to the product of the rate of production of a CF_2Cl_2^* times the rate of attachment of a secondary electron. Since each quantity depends linearly on incident electron current I , the product is proportional to I^2 . This suggestion is also consistent with the observation that the Cl^- yield is enhanced by the Xe spacer layer. The spacer layer may decrease the transmission of secondary electrons from the substrate to the molecular layer, but it can greatly decrease the quenching of $[\text{CF}_2\text{Cl}_2]^*$ and $[\text{CF}_2\text{Cl}_2]^{*-}$ by the metallic substrate, and hence increases the Cl^- yield.

V. CONCLUSIONS

In conclusion, we present observations of negative-ion formation in electron stimulated desorption of adsorbed CF_2Cl_2 molecules on Ru(0001). The TDS results indicate that CF_2Cl_2 is mainly molecularly adsorbed on the substrate at ~ 25 K. At an incident electron energy of 100 eV, the

strong F^- yield shows a maximum around 1 ML of CF_2Cl_2 , while the yield of Cl^- is strongly quenched below 1 ML and remains much lower than the F^- yield even for coverages up to 5 ML. This behavior is contrary to the gas-phase data, where the dominant product is Cl^- . We suggest that the appearance of the F^- yield maximum at nearly the first monolayer may be due to a decrease in transmission of secondary electrons to the topmost CF_2Cl_2 layer with higher coverages, if F^- ions result mainly from attachment of secondary electrons to the molecules via DEA. Furthermore, we observe that a broad structure appears at an incident electron energy of 18.5–20 eV for a multilayer covered surface. This structure is attributed to a core-excited negative-ion resonance resulting from a two-step process: a direct excitation of the molecule by an incident electron and a subsequent capture of a secondary electron from the substrate. The nature of the quenching phenomenon has been discussed in some detail. At low coverages, a molecular orientation effect may lead to a low-desorption efficiency of Cl^- . The image potential effect can also cause the trapping of low-energy Cl^- ions arising from the ground-state single electron resonance at the surface. However, the substrate induced charge-transfer processes may also be responsible for the quenching of core-excited negative-ion resonances.

ACKNOWLEDGMENTS

The authors acknowledge valuable discussions with T. M. Orlando, A. L. Johnson, and N. Hedhili. This work has been supported in part by the National Science Foundation, Grant No. CHE-9705476.

-
- ¹M. J. Molina and F. S. Rowland, *Nature (London)* **249**, 810 (1974).
- ²R. H. Huebner, D. L. Bushnell, Jr., R. J. Celotta, S. R. Mielczarek, and C. E. Kuyatt, *Nature (London)* **257**, 376 (1975).
- ³M. J. Warner, J. L. Bullister, D. P. Wisegarver, R. H. Gammon, and R. F. Weiss, *J. Geophys. Res.* **101**, 20 525 (1996).
- ⁴E. Illenberger, H.-U. Scheunemann, and H. Baumgärtel, *Chem. Phys.* **37**, 21 (1979).
- ⁵P. Rowntree, L. Sanche, L. Parenteau, M. Meinke, and E. Illenberger, *J. Chem. Phys.* **101**, 4248 (1994).
- ⁶St. J. Dixon-Warren, E.-T. Jensen, and J. C. Polanyi, *J. Chem. Phys.* **98**, 5938 (1993).
- ⁷L. Sanche, *Scanning Microsc.* **9**, 619 (1995).
- ⁸E. Illenberger, *Chem. Rev.* **92**, 1589 (1992).
- ⁹G. J. Schulz, *Rev. Mod. Phys.* **45**, 423 (1973).
- ¹⁰*Electron-Molecular Interactions and Their Applications*, edited by L. G. Christophorou (Academic, New York, 1984), Vol. 1.
- ¹¹R. E. Palmer and R. J. Rous, *Rev. Mod. Phys.* **64**, 383 (1992).
- ¹²T. E. Madey, S. A. Joyce, and J. A. Yarmoff, in *Chemistry and Physics of Solid Surfaces VIII*, edited by R. Vanselow and R. Howe (Springer-Verlag, Berlin, 1990), p. 55.
- ¹³L. Nair, N. J. Sack, and T. E. Madey, *Nucl. Instrum. Methods Phys. Res. B* **101**, 79 (1995); N. J. Sack, M. Akbulut, T. E. Madey, P. Klein, H. M. Urbassek, and M. Vicane, *Phys. Rev. B* **54**, 5130 (1996).
- ¹⁴M. Akbulut, T. E. Madey, L. Parenteau, and L. Sanche, *J. Chem. Phys.* **105**, 6043 (1996).
- ¹⁵G. A. Kimmel and T. M. Orlando, *Phys. Rev. Lett.* **77**, 3983 (1996).
- ¹⁶W. C. Simpson, L. Parenteau, R. S. Smith, L. Sanche, and T. M. Orlando, *Surf. Sci.* **390**, 86 (1997).
- ¹⁷M. Meinke and E. Illenberger, *J. Phys. Chem.* **98**, 6601 (1994).
- ¹⁸F. Weik, E. Illenberger, K. Nagesha, and L. Sanche, *J. Phys. Chem. B* **102**, 824 (1998).
- ¹⁹R. Azria, L. Parenteau, and L. Sanche, *Phys. Rev. Lett.* **59**, 638 (1987); L. Sanche, *J. Phys. B* **23**, 1597 (1990).
- ²⁰*CRC Handbook of Chemistry and Physics*, 72nd ed, edited by D. R. Lide (CRC Press, Boston, 1991), pp. 12–99.
- ²¹E. P. Marsh, T. L. Gilton, W. Meier, M. P. Schneider, and J. P. Cowin, *Phys. Rev. Lett.* **61**, 2725 (1988); E. P. Marsh, M. P. Schneider, T. L. Gilton, F. L. Tabares, W. Meier, and J. P. Cowin, *ibid.* **60**, 2551 (1988).
- ²²G. Ertl and J. Küppers, *Low Energy Electrons and Surface Chemistry* (VCH, Weinheim, 1985), p. 147.
- ²³X. L. Zhou, X. Y. Zhu, and J. M. White, *Surf. Sci. Rep.* **13**, 74 (1991).
- ²⁴A. Kiendler, S. Matejcik, J. D. Skalny, A. Stamatovic, and T. D. Märk, *J. Phys. B* **29**, 6217 (1996).
- ²⁵H. Schlichting and D. Menzel, *Surf. Sci.* **272**, 27 (1992).
- ²⁶S. C. Yang, T. M. Chen, C.-R. Wen, Y. J. Hsu, Y. P. Lee, T. J.

- Chuang, and Y. C. Lin, *Surf. Sci.* **385**, L1010 (1997).
- ²⁷H. Sambe, D. E. Ramaker, L. Parenteau, and L. Sanche, *Phys. Rev. Lett.* **59**, 236 (1987).
- ²⁸J. Doucet, P. Sauvageau, and C. Sandorfy, *J. Chem. Phys.* **58**, 3708 (1973).
- ²⁹R. Jadrny, L. Karlsson, L. Mattsson, and K. Siegbahn, *Phys. Scr.* **16**, 235 (1977).
- ³⁰H. W. Jochims, W. Lohr, and H. Baumgärtel, *Ber. Bunsenges. Phys. Chem.* **80**, 130 (1976).
- ³¹K. Wandelt, *J. Vac. Sci. Technol. A* **2**, 802 (1985).
- ³²See, for example, J. Hölzl, F. K. Schulte, and H. Wager, *Solid Surface Physics* (Springer-Verlag, Berlin, 1979), pp. 30, 34, and 35; J. W. Gadzuk and H. Metiu, *Phys. Rev. B* **22**, 2603 (1980); R. Hemmen and H. Conrad, *Phys. Rev. Lett.* **67**, 1314 (1991).
- ³³B. Woratschek, W. Sesselmann, J. Küppers, G. Ertl, and H. Haberland, *Surf. Sci.* **180**, 187 (1987).
- ³⁴W. E. Spicer, *Phys. Rev.* **112**, 114 (1959).
- ³⁵R. L. Lingle, Jr., N.-H. Ge, R. E. Jordan, J. D. McNeill, and C. B. Harris, *Chem. Phys.* **205**, 191 (1996); **208**, 297 (1996).